

RIETVELD TEXTURE REFINEMENT ANALYSIS OF LINDE TYPE A ZEOLITE FROM X-RAY DIFFRACTION DATA

SAMA M. AL-JUBOURI^{1,*}, BASMA I. WAISI¹, STUART M. HOLMES²

¹Department of Chemical Engineering, College of Engineering, University of Baghdad,
Aljadria, Baghdad, P. O. Box 47024, Iraq

²School of Chemical Engineering and Analytical Science, The University of Manchester,
Manchester M13 9PL, United Kingdom

*Corresponding Author: sama.al-jubouri@coeng.uobaghdad.edu.iq

Abstract

Rietveld method was used to conduct a texture refinement analysis for Linde type A zeolite prepared by hydrothermal conditions of 100 °C for 4 h. Material Analysis Using Diffraction software, which is an open access/user-friendly software, was used to accomplish the analysis using the observed X-ray diffraction data. This study shows the feasibility of using Material Analysis Using Diffraction software for zeolite analysis because it has not been applied for zeolite before. Implementation of this software for the texture refinement analysis for zeolite can contribute to the field of zeolite preparation in terms of adding more reliability to the experimental results. The X-ray diffraction results of the prepared zeolite concur well with the standard Linde type A zeolite. All parameters calculated by Rietveld refinement method for the prepared zeolite were close enough to those for the standard zeolite A. Also, ImageJ software was used for image analysis to obtain the average particle size for zeolite A sample.

Keywords: Characterization, Crystal structure, Linde type A zeolite, Rietveld method, Texture analysis, X-ray diffraction.

1. Introduction

Zeolites are crystalline microporous aluminosilicates with an open framework structure of three-dimensional tetrahedral units generating a network of pores and cavities having molecular dimensions [1, 2]. Zeolite structures consist of $[\text{SiO}_4]^{4-}$ and $[\text{AlO}_4]^{5-}$ tetrahedra, which are linked from their corners by shared oxygen atoms [3, 4]. The isomorphous replacement of Si^{4+} by Al^{3+} produces a net negative charge in the framework, which is neutralized by easily exchangeable alkali and alkaline earth metal cations (sodium, potassium, calcium, etc.) occupying the pores and cavities of zeolite [5-9]. Zeolite structure strongly depends on the presence of these inorganic cations within a reaction mixture [10]. The molar composition of SiO_2 and Al_2O_3 are the controlling factor that determines the types of zeolites, which can be produced such as; zeolite A, X, Y, P and sodalite [11].

A was first synthesized by a hydrothermal crystallization process. As explained by Ghasemi et al. [12], Zeolite Linde Type A (LTA) zeolite, NaA zeolite or as called as zeolite A, with an ideal composition of $\text{Na}_{12}\text{Al}_{12}\text{Si}_{12}\text{O}_{48} \cdot 27\text{H}_2\text{O}$, is one of the most important synthesized zeolite. The effective pore diameter depends on the type and position of the compensation cations in zeolite structure [13]. Due to the outstanding properties of LTA zeolite such as adsorption, ion exchange and porosity properties, it is commonly used as adsorbents, ion exchangers (water softeners and, etc.), catalysts and zeolite membranes in various applications such as household products, aquaculture and petrochemical-related industry [14, 15]. According to Xing-dong et al. [16], zeolites properties and utilization in various applications are significantly affected by the morphology and size distribution of zeolite crystals.

Zeolite framework structures, as recognized very early by zeolite scientists, are vital for the understanding of zeolite chemistry. Framework-type has been used to classify zeolitic materials. Basically, a framework type describes the way in which, the tetrahedral atoms (T-atoms) of the framework connect in the highest possible symmetry [17]. Zeolites have economic importance, thus scientists focus their work on the understanding of the crystal structures, the formation of zeolites and finding the relation between crystal structure and properties. Understanding zeolite synthesis processes have gained a great concern as it provides many visions into the mechanism steps. Hence, many important achievements can be resulting in this understanding, such as new zeolites for specific purposes can be produced, new synthesis techniques can be developed and zeolite industrial production can be optimized [18]. It is essential to deeply understand the nucleation and growth processes occurring during zeolite synthesis for the development of improved zeolites structure [19]. Based on a study by Lee et al. [20], the enhancement of the zeolite performance can be conducted by enhancing the zeolite structure characteristics.

X-ray powder diffraction is the most common technique used on a routine basis by the zeolite scientists for determining the zeolite structure as well as its purity. Using a powder diffraction pattern as a “fingerprint” in the identification of synthesis products is the most common application. Several features of a powder diffraction pattern can be of interest to a zeolite scientist as these features can be relatively easily explained to obtain further useful information. The features of powder diffraction pattern can be positions, relative intensities and widths of apparent peaks as well as the pattern background [21, 22]. The structure of microporous molecular sieves can be deduced and refined from high-quality X-ray

powder diffraction data by applying the Rietveld analysis method [17]. H. M. Rietveld in 1967 made an important contribution using X-ray powder patterns to show the possibility of using the whole pattern, including the overlapped lines to refine crystal structures [23].

The Rietveld method is a least-squares refinement, which depends on varying atomic structural, background and peak profile parameters until the calculated pattern best matches the observed pattern (experimental pattern). According to Lutterotti et al. [24] and Wenk et al. [25], literature have presented in different studies that Rietveld texture analysis was also conducted using synchrotron diffraction images and Charge Coupled Devices Camera (CCD) or an image plate detector [26]. Rietveld refinement for texture analysis is meaningfully conducted from powder XRD data because much more information can be elicited than conventional peaks identification methods. Also, it allows characterization of unit cell dimensions, crystallite sizes/shapes, micro-strain in a crystal lattice, atomic coordinates/bond lengths, substitutions/vacancies, phase quantities and texture effects [27, 28].

An accurate powder diffraction intensity data collected at constant step intervals of 2θ , a starting model that is reasonably close to the actual crystal structure and a model that accurately describes the peak shape and width as a function of 2θ are the essential requirements for a Rietveld structure refinement [29]. For zeolite structure analysis, the Rietveld method has been successfully applied to solve a great number of structural problems concerning zeolite frameworks topology, occupancies of cation sites, coordinates of the lattice, the templates or guest molecules position and the position of clusters introduced into the structure [30]. The quantity minimized in a Rietveld refinement is given by values called R-factor Eq. (1):

$$R = \sum_i w_i (Y_{io} - Y_{ic})^2 \quad (1)$$

where Y_{io} and Y_{ic} are the observed and calculated intensities at step i (the 2θ angle) and w_i is the weight given to step i , which generally equals the square root of the observed intensity. The observed intensity at each step in a diffraction pattern consists of contributions from Bragg peaks and the background at that step [29]. A reasonably good starting model of the zeolite structure is required to conduct the fitting process as the system has a high degree of freedom with respect to the parameters that can be varied such as, unit cell parameters, preferred orientation, atomic coordinates and parameters of the profile function [17].

Other quantities namely R_p , R_e , R_{wp} and X Eq. (2) to (5) respectively are used to evaluate the progress of a Rietveld refinement and the agreement between the measured and calculated patterns.

$$R_p = \frac{\sum_i |Y_{io} - Y_{ic}|}{\sum_i Y_{io}} \quad (2)$$

$$R_e = \sqrt{\frac{n-p}{\sum_i w_i Y_{io}^2}} \quad (3)$$

$$R_{wp} = \sqrt{\frac{\sum_i w_i (Y_{io} - Y_{ic})^2}{\sum_i w_i Y_{io}^2}} \quad (4)$$

$$X = \frac{R_{wp}}{R_e} \quad (5)$$

where the numerator of R_{wp} is the function being minimized, so R_{wp} is the most significant agreement factor and it has values below 12% for typical adequate refinements. The “expected” R index (R_e) can be defined for n total observations with a model that has p parameters. The X index is the ratio of R_{wp} to R_e , known as the fit goodness, which is used to measure how well the calculated model matches the observed data [29].

In case of perfect refinement and correct weighted data, X value has to be 1. When the parameters justified by the quality of the data are less than the parameters that the model has, the value of X has to be less than 1. However, the inappropriate model is indicated by X value of 1.7. Evaluating the quality of a refinement data also requires examination of different plots and chemically reasonable values of bond angles, bond lengths (or coordination distances) and occupancy factors of the atoms in the final structure [17, 29]. Rietveld method has been implemented with General Structure Analysis System (GSAS), but this implementation is restricted with a limited number of crystal structures [31]. However, Rietveld method via Analysis Using Diffraction (MAUD) software package, which is freely affordable software based on JAVA, grants sophisticated Rietveld analysis and algorithms for desired orientation [32]. It has been a challenge and target for zeolite scientists to discover new phases of zeolite with comprehensive information about crystal structure characteristics and frameworks topology.

This work deals with Rietveld refinement analysis conducted for LTA zeolite using X-ray diffraction data with a special focus on the methods of structure solution. MAUD software was used for Rietveld refinement analysis to obtain specific structural characteristics of LTA zeolite crystals. ImageJ software was also used for SEM image analysis.

2. Experimental work

2.1. Chemicals

The chemicals, which were used in this work were hydrous sodium metasilicates ($\text{Na}_2\text{SiO}_3 \cdot 9\text{H}_2\text{O}$ from Acros Organic), anhydrous sodium aluminate (55-56% wt Al_2O_3 from Riedel-deHaën), sodium hydroxide (NaOH pellets 99.9% wt from Fisher Scientific) and deionized water.

2.2. Preparation and characterization of zeolite A

The literature presents a somewhat wide range of reaction compositions, which have been used to prepare zeolite A. As mentioned by Howell [33], Zeolite A with a gel composition of 4.145 Na_2O : 1 Al_2O_3 : 2 SiO_2 : 240 H_2O was prepared according to the ranges; $\text{SiO}_2/\text{Al}_2\text{O}_3$ of 0.8-3, $\text{Na}_2\text{O}/\text{SiO}_2$ of 1.3-2.5 and $\text{H}_2\text{O}/\text{Na}_2\text{O}$ of 35-200. As reported by Robson [34], the hydrothermal method used to prepare zeolite A was approximately based on the procedures. The mother gel was prepared by dissolving 0.347 g of sodium hydroxide pellets in 20 g deionized water and then the produced solution was divided into two equal parts. The first part was gently mixed with 2.793 g hydrous sodium metasilicates while the second part was mixed with 0.914 g anhydrous sodium aluminate. After 15-30 min, silica solution was poured into the alumina solution and left under homogeneously mixing for 20-30 min until formation of a thick creamy gel. Then the produced gel was placed in a Teflon-lined autoclave and crystallized at 100 °C for 4 h. After quenching of the

autoclave, the product was recovered, filtered, washed with deionized water until the pH of the washing solution goes below 9 and then dried at 50-80 °C. The sample of the synthesized zeolite was characterized by X-ray Powder Diffraction (XRD), Scanning Electron Microscopy (SEM) and Energy Dispersive Analysis by X-ray (EDAX).

The characterization of zeolite was conducted using model Miniflex by Rigaku X-ray analytical instrumentation with CuK α radiation source ($\lambda = 1.5418 \text{ \AA}$), voltage = 30 kV, current = 30 mA, step size = 0.03°, scan speed = 3° min⁻¹, $2\theta = 5\text{-}45^\circ$ and total time ~ 20 min. SEM and EDAX measurements were conducted using model FEI Quanta 200. The sample was coated with gold by a sputter coater for SEM imaging, while EDAX analysis was carried out without coating the sample.

3. Results and Discussion

Figure 1 shows the XRD pattern of zeolite A prepared, where, 26 peaks were identified from this figure for conducting texture refinement analysis via Rietveld method. As shown in Fig. 1, all peaks present are sharp with well-defined diffraction at all the range of 2θ indicating a high degree of crystallinity and structurally ordered product.

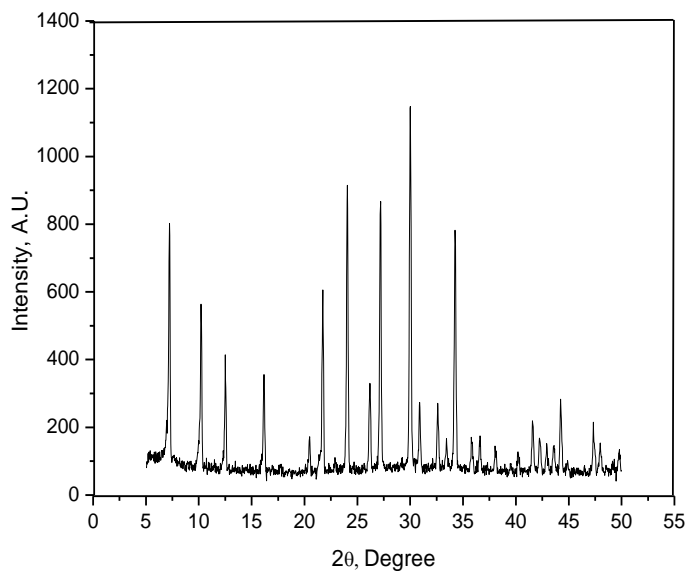


Fig. 1. XRD pattern of 4A zeolite crystallized at 100 °C for 4 h.

The morphology of the synthesized zeolite A is shown in Fig. 2, which presents the SEM image of the prepared sample. The zeolite sample shows a distinct cubic morphology with sharp edges. Based on studies on ImageJ [35], the particle size of zeolite crystals was analysed from the SEM image using ImageJ software (National Institute of Health). The ImageJ software is user-friendly open source software, which is used for image analysis. The image was first adjusted as shown in Fig. 3 using the software, where the background appears in a white colour and the crystals appear in a black colour. The average particle size of zeolite was found as 2968 Å.

The results of the elemental analysis conducted for zeolite A sample by EDAX are listed in Table 1. Where the Si/Al ratio of the sample was 1.14 with a standard deviation of 0.008.

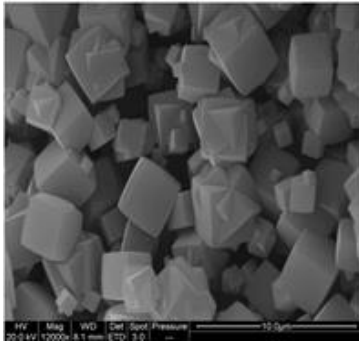


Fig. 2. SEM image of 4A zeolite crystallized at 100°C for 4 h.

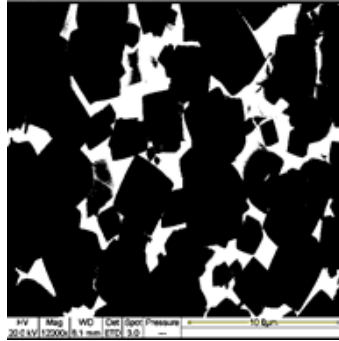


Fig. 3. SEM image of 4A zeolite modified by ImageJ software.

Table 1. Elemental analysis of zeolite a conducted by EDAX.

Element	Si	Al	Na	O	Si/Al
Wt. %	22.154	19.41	11.844	46.59	1.1412
Standard deviation	0.533	0.334	0.915	0.690	0.008

As stated by Lutterotti [36], the characterization of zeolite crystal structure was conducted via Rietveld refinement method combined with MAUD software, version 2.26, which was used for the analysis. The Rietveld method uses the calculated diffraction patterns to model the crystal structure [28]. Rietveld texture analysis using MAUD software is mainly based on X-Ray diffraction data and it generates a feasible separation of the overlapping peaks, therefore, it resolves the problem of imprecise determination of structure resulting from the broad and totally overlapped diffraction peaks [27, 28]. Consequently, appearing of noise and absence of clarity in the XRD data and extensively overlapped peaks is the major drawbacks of this method. The calculated patterns with the adjusted measured pattern data of the prepared zeolite provide the structural parameters and the diffraction profile. According to the Structure Commission of the International Zeolite Association (IZA-SC) [37], Zeolite Structures database were refined with the standard zeolite data. The adjusted parameters were lattice parameters (a), atomic positions and occupancy. The refined parameters were the scale factor, background (Pi), shift lattice parameters, profile half-width parameters, isotropic displacement parameters and strain anisotropy factor. A four-degree polynomial, shown in Eq. (6), was used as the background function suggested by MAUD software. The constant values of the modified background are listed in Table 2. The data were drawn with a linear intensity scale mode and the least square method was used for the fitting.

$$P = b_0 + b_1X + b_2X^2 + b_3X^3 + b_4X^4 \quad (6)$$

Reed and Breck [38] solved the LTA zeolite crystal structure with space group Pm₃m with a $\frac{1}{4}$ 12.3Å. Later, Gramlich and Meier [39] showed that the LTA zeolite is better described in space group Fm₃c with a $\frac{1}{4}$ 24.6Å. The pseudo-voigt function was used to model the peak profile [40] and it was carried out with space

group Fm_33c. Le Bail [41] applied the structure-independent approach for this purpose, by which, the Rietveld refinements in this work focuses on the determination of the lattice parameter. The lattice parameter is presented in Table 2.

Values of R index were calculated by the software to check the quality of the refinement for the Rietveld refinement method. The calculated R index values listed in Table 2 were less than 0.15, which indicates a good refinement result. There were no impurities detected in the prepared zeolite as given by software where the sample was 100% LTA zeolite. Figure 4 shows a comparison between the observed pattern of the sample and the fitted data obtained using MAUD software. The red line is the fitted formula of the least square method, while the peak position of the reference and the prepared sample is below the diffraction pattern. Figure 4 also exhibits a good data fitting between the pattern and the fitting profile.

Bosnar et al. [10] and Bronic et al. [42] obtained the density of the prepared zeolite, which was refined from the standard zeolite A database file. It has a value of 2.01879 g/cm^3 compared with 2 g/cm^3 . The cell length of the sample crystal was 24.614 \AA , while cell length for the standard zeolite crystal was 24.6 \AA with an error of 5%. A comparison between a standard zeolite A and a prepared zeolite A based on the values and error estimated for the refinement method is presented in Table 3. Popa [43] rule is a compatible approach with the Rietveld refinement method, which was used to calculate the crystal size and microstrain for anisotropic crystal. Popa model approach for the anisotropic microstructure analysis has a value of -0.001115088 with an error% of 2.2928756 E-4 . The particle crystallite sizes of catalysts were calculated in the assumption of the isotropic model, it was equal to 3143.734 \AA . Figure 5 shows the lattice crystal predicted by the MAUD software; where it shows a cubic structure with molecules distributed all over the lattice.

Table 2. Values of parameters and error estimated for the refinement method.

Parameter type	Symbol	Value	Error%
Background	P_0	178.63431	6.6147556
	P_1	-17.46209	1.3438451
	P_2	0.9770485	0.09012897
	P_3	0.022221243	0.002404153
Cell length, A	a	24.6	5
Lattice angle	-	90	0
R index	R_{wp}	0.14296974	-
	R_p	0.11070305	-

Table 3. The values of parameters and error estimated for the refinement method.

Parameter type	Standard zeolite A	Prepared zeolite A
Fm	_33c	_33c
Cell length, A	24.6	24.614
Density, g/cm³	2	2.01879

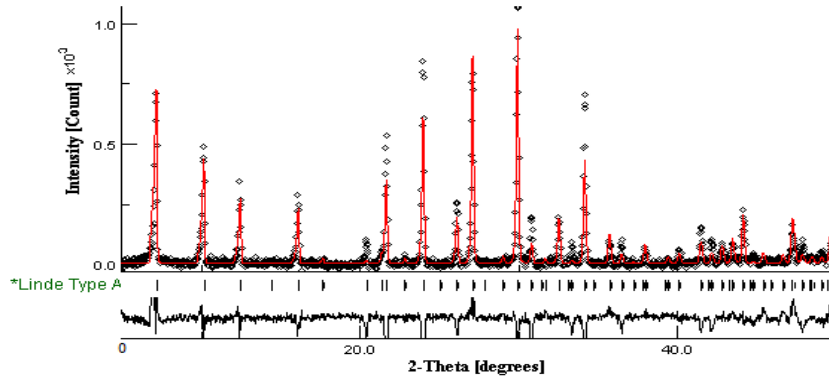


Fig. 4. A comparison between the observed pattern and the fitted data obtained using MAUD software.

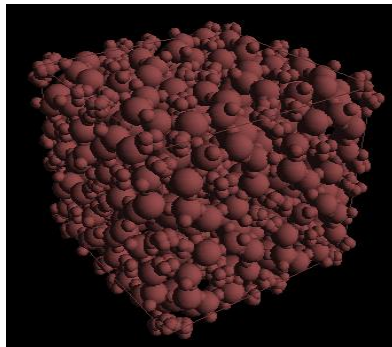


Fig. 5. Predicted crystal shape of LTA zeolite given by MAUD software.

4. Conclusions

The results introduced in this work show the feasibility of using MAUD software for zeolite analysis, which has not been applied for zeolite before. Rietveld refinement method using MAUD successfully confirmed preparation of pure zeolite A by hydrothermal treatment. The XRD results of the prepared zeolite matched well with that of standard LTA zeolite. All parameters that calculated using the Rietveld refinement method was close enough to the standard zeolite A. Zeolite particle size obtained using Rietveld refinement was very close to the value of particle size obtained via ImageJ software.

Nomenclatures

a	Lattice parameters or Cell length, A
P_o	Background parameter
P_1	Background parameter
P_2	Background parameter
R	R-factor
R_e	The expected R index
R_p	R index based on Eq. (2)
R_{wp}	R index based on Eq. (4)
w_i	Weight given to step i
Y_{io}	Observed intensities at step i
Y_{ic}	Calculated intensities at step i
X	Fit goodness

Greek Symbols

θ	Angle of reflection, Deg.
λ	Wave length, A

Abbreviations

CCD	Charge Coupled Devices
EDAX	Energy Dispersive Analysis by X-ray
GSAS	General Structure Analysis System
IZA-SC	Structure Commission of the International Zeolite Association
LTA	Lined Type A
MAUD	Material Analysis using Diffraction
SEM	Scanning Electron Microscopy
XRD	X-ray Diffraction

References

1. Breck, D.W. (1974). *Zeolite molecular sieves: Structure, chemistry and use*. New York: Wiley-Interscience.
2. Schwanke, A.J.; Balzer R.; and Pergher S. (2017). *Microporous and mesoporous materials from natural and inexpensive sources*. Handbook of Ecomaterials. Cham, Switzerland: Springer International Publishing.
3. Gougazeh, M.; and Buhl, J.-C. (2014). Synthesis and characterization of zeolite A by hydrothermal transformation of natural Jordanian kaolin. *Journal of the Association of Arab Universities for Basic and Applied Sciences*, 15, 35-42.
4. Zhang, X.; Tong, D.; Jia, W.; Tang, D.; Li, X.; and Yang, R. (2014). Studies on room-temperature synthesis of zeolite NaA. *Materials Research Bulletin*, 52, 96-102.
5. Nibou, D.; Mekatel, H.; Amokrane, S.; Barkat, M.; and Trari, M. (2010). Adsorption of Zn^{2+} ions onto NaA and NaX zeolites: Kinetic, equilibrium and thermodynamic studies. *Journal of Hazardous Materials*, 173(1-3), 637-646.

6. Ibrahim, H.S.; Jamil, T.S.; and Hegazy, E.Z. (2010). Application of zeolite prepared from Egyptian kaolin for the removal of heavy metals: II. Isotherm models. *Journal of Hazardous Materials*, 182(1-3), 842-847.
7. Jamil, T.S.; Ibrahim, H.S.; El-Maksoud, I.H.A.; and El-Wakeel, S.T. (2010). Application of zeolite prepared from Egyptian kaolin for removal of heavy metals: I. Optimum conditions. *Desalination*, 258(1-3), 34-40.
8. De Haro-Del Rio, D.A.; Al-Jubouri, S.M.; and Holmes, S.M. (2017). Hierarchical porous structured zeolite composite for removal of ionic contaminants from waste streams. *Chimica Oggi - Chemistry Today*, 35(3), 56-58.
9. Inagaki, S.; Thomas, K.; Ruaux, V.; Clet, G.; Wakihara, T.; Shinoda, S.; Okamura, S.; Kubota, Y.; and Valtchev, V. (2014). Crystal growth kinetics as a tool for controlling the catalytic performance of a FAU-type basic catalyst. *ACS Catalysis*, 4(7), 2333-2341.
10. Bosnar, S.; Antonic-Jelic, T.; Bronic, J.; Krznaric, I.; and Subotic, B. (2004). Influence of anions on the kinetics of zeolite A crystallization: A population balance analysis. *Journal of Crystal Growth*, 267(1-2), 270-282.
11. Garcia, G.; Cabrera, S.; Hedlund, J.; and Mouzon, J. (2018). Selective synthesis of FAU-type zeolites. *Journal of Crystal Growth*, 489, 36-41.
12. Ghasemi, M.; Javadian, H.; Ghasemi, N.; Agarwal, S.; and Gupta, V.K. (2016). Microporous nanocrystalline NaA zeolite prepared by microwave assisted hydrothermal method and determination of kinetic, isotherm and thermodynamic parameters of the batch sorption of Ni (II). *Journal of Molecular Liquids*, 215, 161-169.
13. Melo, C.R.; Riella, H.G.; Kuhnen, N.C.; Angioletto, E.; Melo, A.R.; Bernardin, A.M.; da Rocha, M.R.; and da Silva, L. (2012). Synthesis of 4A zeolites from kaolin for obtaining 5A zeolites through ionic exchange for adsorption of arsenic. *Materials Science and Engineering: B*, 177(4), 345-349.
14. Zhang, X.; Tang, D.; and Jiang, G. (2013). Synthesis of zeolite NaA at room temperature: The effect of synthesis parameters on crystal size and its size distribution. *Advanced Powder Technology*, 24(3), 689-696.
15. Reinoso, D.; Adrover, M.; and Pedernera, M. (2018). Green synthesis of nanocrystalline faujasite zeolite. *Ultrasonics Sonochemistry*, 42, 303-309.
16. Xing-dong, L.; Yi-pin, W.; Xue-min, C.; Yan, H.; and Jin, M. (2013). Influence of synthesis parameters on NaA zeolite crystals. *Powder Technology*, 243, 184-193.
17. Jacobs, P.A.; Flanigen, E.M.; Jansen, J.C.; and van Bekkum, H. (2001). *Introduction to zeolite science and practice*, vol. 137 (2nd ed.). Amsterdam, Netherlands: Elsevier Science B.V.
18. Loiola, A.R.; Andrade, J.C.R.A.; Sasaki, J.M.; and da Silva, L.R.D. (2012). Structural analysis of zeolite NaA synthesized by a cost-effective hydrothermal method using kaolin and its use as water softener. *Journal of Colloid and Interface Science*, 367(1), 34-39.
19. Aguilar-Mamani, W.; Akhtar, F.; Hedlund, J.; and Mouzon, J. (2018). Solution-mediated growth of NBA-ZSM-5 crystals retarded by gel entrapment. *Journal of Crystal Growth*, 487, 57-64.

20. Lee, W.; Lee, T.; Jang, H.-G.; Cho, S.J.; Choi, J.; and Ha, K.-S. (2018). Effects of hierarchical zeolites on aromatization of acetylene. *Catalysis Today*, 303, 177-184.
21. Auerbach, S.M.; Carrado, K.A.; and Dutta, P.K. (2003). *Handbook of zeolite science and technology*. New York, Basel: Marcel Dekker, Inc.
22. Cejka, J.; van Bekkum, H.; Corma, A.; and Schuth, F. (2007). *Introduction to zeolite science and practice*, vol. 168 (3rd revised ed.). Oxford, United Kingdom: Elsevier B.V.
23. Woolfson, M.M. (1997). *An introduction to X-ray crystallography*. Cambridge, New York: Cambridge University Press.
24. Lutterotti, L.; Vasin, R.; and Wenk, H.-R. (2014). Rietveld texture analysis from synchrotron diffraction images. I. Calibration and basic analysis. *Powder Diffraction*, 29(1), 76-84.
25. Wenk, H.-R.; Lutterotti, L.; Kaercher, P.; Kanitpanyacharoen, W.; Miyagi, L.; and Vasin, R. (2014). Rietveld texture analysis from synchrotron diffraction images. II. Complex multiphase materials and diamond anvil cell experiments. *Powder Diffraction*, 29(3), 220-232.
26. Aranda, M.A.G. (2016). Recent studies of cements and concretes by synchrotron radiation crystallographic and cognate methods. *Crystallography Reviews*, 22(3), 150-196.
27. Rietveld, H.M. (1967). Line profiles of neutron powder - diffraction peaks for structure refinement. *Acta Crystallographica*, 22(1), 151-152.
28. Rietveld, H.M. (1969). A profile refinement method for nuclear and magnetic structures. *Journal of Applied Crystallography*, 2(2), 65-71.
29. Chester, A.W.; and Derouane, E.G. (2009). *Zeolite characterization and catalysis*. Dordrecht, Netherlands: Springer Science & Business Media B.V.
30. Weitkamp, J.; and Puppe, L. (1999). *Catalysis and zeolites*. Germany: Springer-Verlag Berlin Heidelberg GmbH.
31. Larson, A.C.; and Von Dreele, R.B. (1986). GSAS: General structure analysis system. *Los Alamos National Laboratory Report LAUR 86-748*.
32. Lutterotti, L.; Matthies, S.; and Wenk, H.-R. (1999). MAUD (Material Analysis Using Diffraction): A user friendly Java program for texture analysis and more. *Proceedings of the Twelfth International Conference on Textures of Materials*. Montreal, Canada, 1599-1604.
33. Howell, P.A. (1963). Process for producing molecular sieves. United States Patent Office, 3,101,251.
34. Robson, H. (2001). *Verified synthesis of zeolitic materials*. Amsterdam: The Netherlands: Elsevier Science B.V.
35. ImageJ. (2018). Image processing and analysis in Java. Retrieved April 17 , 2018 from <https://imagej.nih.gov/ij/index.html>.
36. Lutterotti, L. (2010). Total pattern fitting for the combined size-strain-stress-texture determination in thin film diffraction. *Nuclear Instruments and Methods in Physics Research Section B: Beam Interactions with Materials and Atoms*, 268(3-4), 334-340.

37. Structure Commission of the International Zeolite Association (IZA-SC). (2017). Database of zeolite structures. Retrieved November 2, 2017 from <http://www.iza-structure.org/databases/>.
38. Reed, T.B.; and Breck, D.W. (1956). Crystalline zeolites. II. Crystal structure of synthetic zeolite, type A. *Journal of the American Chemical Society*, 78(23), 5972-5977.
39. Gramlich, V.; and Meier, W.M. (1971). The crystal structure of hydrated NaA : A detailed refinement of a pseudo symmetric zeolite structure. *Zeitschrift für Kristallographie - Crystalline Materials*, 133(1-6), 134-149.
40. Thompson, P.; Cox, D.E.; and Hastings, J.B. (1987). Rietveld refinement of Debye-Scherrer synchrotron X-ray data from Al₂O₃. *Journal of Applied Crystallography*, 20, 79-83.
41. Le Bail, A. (2005). Whole powder pattern decomposition methods and applications: A retrospection. *Powder Diffraction*, 20(4), 316-326.
42. Bronic, J.; Muzic, A.; Jelic, T.A.; Kontrec, J.; and Subotic, B. (2008). Mechanism of crystallization of zeolite A microcrystals from initially clear aluminosilicate solution: A population balance analysis. *Journal of Crystal Growth*, 310(22), 4656-4665.
43. Popa, N.C. (1998). The (hkl) dependence of diffraction-line broadening caused by strain and size for all Laue groups in Rietveld refinement. *Journal of Applied Crystallography*, 31, 176-180.